



Analysis of compartmental models of ligand-induced endocytosis

Abraham R. Tzafiriri^{a,*}, David Wu^a, Elazer R. Edelman^{a,b}

^a *Harvard-MIT Division of Health Sciences and Technology, Massachusetts Institute of Technology, Room 16-343, Cambridge, MA, USA*

^b *Cardiovascular Division, Brigham and Women's Hospital, Harvard Medical School, Boston, MA, USA*

Received 24 October 2003; received in revised form 4 March 2004; accepted 12 March 2004

Abstract

Kinetic models have played a pivotal role in the study of ligand-induced endocytosis. However, an analysis that suggests a systematic way to validate such models is lacking. The current work analyses the base model of ligand-induced endocytosis for three widely used experimental protocols. In protocol I cells initially devoid of ligand are incubated in ligand solution, whereas protocols II and III are desorption experiments in which an initial pool of surface or internalized ligand–receptor complexes, respectively, are released into an elution medium that is initially devoid of ligand. A short-time analysis of protocol I using successive substitutions yielded a corrected pre-factor for the In/Sur plot introduced by Wiley and Cunningham (Cell 25 (1981) 433). In contrast, neglecting the variation in receptor numbers yielded an approximation of protocol I that is valid for long times (e.g. tens of minutes). Similarly, the low cell-concentration limits of protocols II and III are derived by neglecting the concentration of free ligand. The simplicity of these approximations provides a simple and reliable method for estimating the parameters governing ligand kinetics, while their definitive nature implies that they can be used to verify the validity of the base model. This analysis also provides insight on the fast endocytosis and recycling limit of protocol III.

© 2004 Elsevier Ltd. All rights reserved.

Keywords: Analytical approximations; Initial transient; Linear stability; In/Sur plot; Growth factors

1. Introduction

Most models of cellular pharmacokinetics are based on an analogy between receptor and enzyme kinetics and employ kinetic equations to describe a small number of rate limiting steps between various cellular compartments (Levitzki, 1984; Lauffenburger and Linderman, 1993; Mukherjee et al., 1997; Wiley et al., 2003). In addition to numerical simulations of these models, their relative simplicity has prompted the derivation of simple analytical approximations for purposes of parameter estimation and model validation (Wiley and Cunningham, 1981, 1982; Zigmond et al., 1982; Shimizu and Kawashima, 1989). Motivated by the analogy to enzyme kinetics, Wiley and Cunningham (1981) employed the quasi-steady-state approximation to derive a graphical method for parameter estimation. These authors also introduced the In/Sur plot as a means of estimating the endocytosis rate constant from

simple ligand sorption experiments (Wiley and Cunningham, 1982). A major limitation of the In/Sur plot is that it is only valid for short times such that degradation and recycling terms are negligible compared to the endocytosis and binding terms.

As the number of parameters in receptor signaling models increases, numerical techniques for parameter estimation are increasingly employed (Waters et al., 1990; Schoeberl et al., 2002; Swameye et al., 2003). However, this approach has two limitations. First, just as in enzyme kinetics, the stiffness of these models implies that only a subset of the parameters can be estimated simultaneously for a given experiment. This is because by its very definition stiffness implies the existence of a hierarchy of time scales (Heinrich et al., 1977; Schauer and Heinrich, 1979; Roussel and Fraser, 1991). Consequently, most experiments only capture the slow quasi-steady-state kinetics of stiff systems. In the absence of a good characterization of the kinetic equations it is impossible to plan a logical experimental strategy for parameter fitting and a brute force numerical approach may require many experimental permutations. Second, a fully numerical approach of

*Corresponding author. Tel.: +1-617-252-1655; fax: +1-617-253-2514.

E-mail address: ramitz@mit.edu (A.R. Tzafiriri).

simultaneously estimating all the parameters does not validate the model. This realization has motivated a renewed effort to derive analytical approximations for simple enzyme kinetics models (Schnell and Mendoza, 1997, 2000a, 2000b; Schnell and Maini, 2000; Tzafriri et al., 2002; Tzafriri, 2003; Tzafriri and Edelman, 2004). Despite their analogy to enzyme kinetics models, endocytosis models are not as well studied.

In this work, we analyse the base model of ligand-induced endocytosis (Lauffenburger and Linderman, 1993) for three widely used experimental protocols. Protocol I is a ligand uptake experiment into cells that are initially devoid of ligand, whereas Protocols II and III are desorption experiments from cells that were pre-loaded with surface and internalized ligand–receptor complex, respectively. Our analysis of these experiments relies heavily on the sequence of physical processes occurring in each of these experimental protocols (Hill, 1942; Buchman and Parnas, 1994). The sequential nature of these kinetic models is shown to dictate the sensitivity of each of the experimental protocols to the various model parameters. In turn, this enabled us to derive *controlled* approximate solutions to the base model for each of these protocols. In this context the term *controlled* refers to the existence of a well-defined criterion for the validity of a given approximation.

2. The base model

In the current work we shall restrict our discussion to the base model depicted in Fig. 1. Although an idealization, this model accounts for all the essential processes governing cellular pharmacokinetics: ligand binding to surface receptors, constitutive and ligand induced endocytosis, receptor recycling and degradation. Applying the law of mass action to this compartmental scheme translates it into the following set of coupled differential equations:

$$\dot{L} = (-k_f LR_s + k_r C_s)(n/N_{av}), \quad (1)$$

$$\dot{C}_s = k_f LR_s - (k_r + k_e)C_s + (1 - f_1)k_{rec} C_i, \quad (2)$$

$$\dot{C}_i = k_e C_s - ((1 - f_1)k_{rec} + f_1 k_{deg})C_i, \quad (3)$$

$$\dot{R}_s = -k_f LR_s + k_r C_s + V_r - k_t R_s + (1 - f_2)k_{rec} R_i, \quad (4)$$

$$\dot{R}_i = k_t R_s - ((1 - f_2)k_{rec} + f_2 k_{deg})R_i, \quad (5)$$

where over-dots denote temporal differentiation, L denotes the extracellular concentration of free ligand, R_s and R_i denote the numbers of unoccupied surface and intracellular receptors, respectively, C_s and C_i denote the numbers of ligand-bound surface and intracellular receptors, respectively, f_1 and f_2 are, respectively, the fractions of ligand-bound and unoccupied internalized receptors that are sorted to degrada-

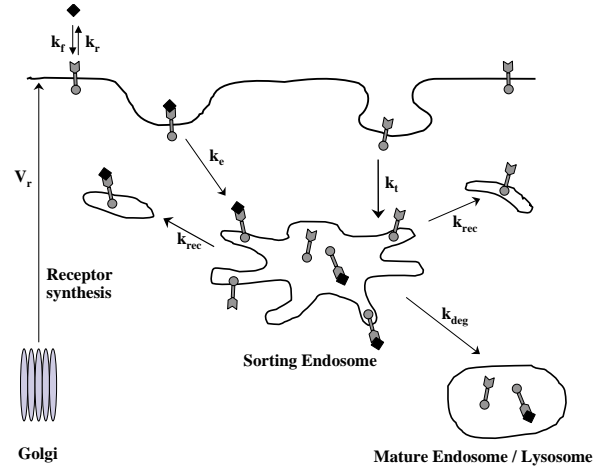


Fig. 1. Rate limiting trafficking steps considered in the base model. Extracellular ligand (\square) binds reversibly to free surface receptor (\odot) with on rate k_f and off rate k_r . Ligand–receptor complexes (\odot) are endocytosed with an average rate constant k_e . Free receptors are also internalized, but with a slower constitutive rate constant k_t . Internalized free and ligand-bound receptors meet in the sorting endosome. A fraction of internalized receptors are pinched off along with tubular buds of the sorting endosome and recycle back to the plasma membrane with an average rate constant k_{rec} . The remaining fraction of internalized receptors degrades in the maturing endosome and eventually in the lysosome. This degradation is assumed to be first order with an average rate constant k_{deg} . New receptors are continually synthesized in the Golgi and brought to the cell surface at a rate V_r . This base model only considers the rate limiting steps for growth factor induced endocytosis and neglects fast processes such as dimerization of surface receptors, activation of occupied receptors and binding to surface proteins, etc. (Lauffenburger and Linderman, 1993; Mukherjee et al., 1997).

tion, n denotes the cell density (cells/l), N_{av} is the Avogadro number and the rate constants are defined in Fig. 1. We will consider the solution of these equations under three different initial conditions, corresponding to each of the three experimental protocols.

Protocol I: Cells are incubated in binding medium at 37°C. Prior to incubation the cells are devoid of ligand. The initial conditions corresponding to this protocol are therefore

$$(L, R_s, C_s, C_i, R_i) = (L_0, R_{s0}, 0, 0, R_{i0}), \quad t = 0, \quad (6a)$$

where

$$R_{s0} \equiv \left(\frac{V_r}{k_t} \right) \left(1 + \frac{(1 - f_2)k_{rec}}{f_2 k_{deg}} \right), \quad R_{i0} \equiv \frac{V_r}{f_2 k_{deg}} \quad (6b, c)$$

are the steady-state pre-incubation receptor numbers.

Protocol II: Cells are equilibrated with labeled ligand at 4°C. The low temperature prevents the internalization of ligand–receptor complexes (Lauffenburger and Linderman, 1993). At the end of the incubation period, the cells are quickly washed with ice-cold salt solution to remove unbound ligand and are then transferred to a pre-warmed water bath (37°C) in which they are incubated for various times. At the end of the timed

incubations the cell plates are removed from the water bath and the medium containing the dissociated ligand is sampled. The initial conditions corresponding to this protocol are therefore

$$(L, R_s, C_s, C_i, R_i) = (0, R_{s2}, C_{s2}, 0, R_{i2}), \quad t = 0. \quad (7)$$

Protocol III: Similar to protocol I except that after pre-incubation in the warm binding medium cells are washed in a cold mild acid solution in order to remove the surface bound ligand (Lauffenburger and Linderman, 1993) and are subsequently transferred to a pre-warmed water bath (37°C) in which they are incubated for various times and the concentrations are measured just as in Protocol II. The initial conditions corresponding to this protocol are therefore

$$(L, R_s, C_s, C_i, R_i) = (0, R_{s3}, 0, C_{i3}, R_{i3}), \quad t = 0. \quad (8)$$

3. Analysis

In the following sections we derive approximate solutions for protocols I–III. Fig. 2 is a schematic representation of the initial conditions corresponding to each of these protocols. Gray cells depict compartments initially devoid of ligand, while black cells depict ligand-pre-loaded compartments. This representation emphasizes that all three protocols are relaxation experiments from a single compartment to its nearest neighbors. This unifying view will guide our analysis of these protocols.

3.1. Protocol I

Although Eqs. (1)–(6) cannot be solved in closed form, at least for short times their solution can be approximated to arbitrary accuracy using the method of successive substitutions (Lin and Segel, 1988; Hill,

1942). Such an analysis is carried out in Appendix B where we find that

$$\frac{C_i}{C_s} = \left(\frac{k_e}{2}\right)t + O(t^2). \quad (9)$$

This result is of consequence for the simplest variant of the In/Sur plot (e.g. C_i/C_s versus time) and shows that the initial slope in such plots corresponds to $k_e/2$ and not to k_e as is commonly believed (Wiley and Cunningham, 1982; Helin and Beguinot, 1991; Fannon and Nugent, 1996; Sorkina et al., 2002). Another obvious limitation of the In/Sur plot is that it is based on a very short-lived approximation that limits its application to very short experimental times, and consequently to a small number of experimental points. This limitation has prompted the derivation of the refined In/Sur plot (Opresko and Wiley, 1987). However, the latter refinement is also restricted to short times, before recycling and degradation have significant impact. Vuk-Pavlovic and co-workers derived approximate analytical solutions of the base model for protocol I under conditions of excess ligand concentration (Myers et al., 1987; Bajzer et al., 1989). Although their derivations are mathematically sound, they are nevertheless incompatible with an underlying assumption of the base model, that ligand concentration is sufficiently low not to saturate the different pathways. This is the justification for using first-order processes to model the kinetics of influx and efflux into the various cellular compartments.

3.1.1. Excess receptor concentration

As shown in Appendix A, Eqs. (1)–(5) have a single steady-state point

$$(L, R_s, C_s, C_i, R_i) = (0, R_{s0}, 0, 0, R_{i0}), \quad (10)$$

which is also the equilibrium state. Consequently, protocol I represents a perturbation of the system from its equilibrium, which subsequently relaxes to the initial state. When the receptor number is in great excess of the ligand

$$\delta \equiv \frac{L_0}{R_{s0}(n/N_{av})} \ll 1, \quad (11)$$

the perturbation is small and the system is well characterized by its linear response.

However, the equations describing the system's linear response are still rather complicated and unilluminating (see Appendix A). In this section, we therefore limit our analysis to *non-recycling* receptors, $f_1 = f_2 = 1$, in which case (as derived in Appendix A) the linear response of Eqs. (1)–(5) is given by

$$\dot{L} \approx (-k_a L + k_r c_s), \quad (12)$$

$$\dot{c}_s \approx k_a L - (k_r + k_e) c_s, \quad (13)$$

$$\dot{c}_i = k_e c_s - k_{deg} c_i, \quad (14)$$

Protocol \ Compartment	I	II	III
Extracellular			
Cell Surface			
Intracellular			

Fig. 2. Initial conditions corresponding to protocols I–III. Gray cells depict compartments initially devoid of ligand, while black cells depict ligand-replete compartments. This schematic representation emphasizes that in all three protocols the contents of a single compartment are relaxing into nearest neighbor compartments.

$$\dot{r}_s \approx -k_a L + k_r c_s - k_t r_s, \quad (15)$$

$$\dot{r}_i = k_t r_s - k_{deg} r_i, \quad (16)$$

where we introduced the simplifying notations

$$k_a \equiv k_f R_{s0}(n/N_{av}), \quad (17)$$

$$c_s \equiv C_s(n/N_{av}), \quad c_i \equiv C_i(n/N_{av}), \quad (18a, b)$$

$$r_s \equiv (R_s - R_{s0})(n/N_{av}), \quad r_i \equiv (R_i - R_{i0})(n/N_{av}). \quad (18c, d)$$

These definitions imply the following initial conditions:

$$(L, c_s, c_i, r_s, r_i) = (0, 0, 0, 0, 0), \quad t = 0. \quad (19)$$

Solving Eqs. (12)–(16) subject to initial conditions (19) we find

$$L \approx \left(\frac{L_0}{\lambda_+ - \lambda_-} \right) \left((\lambda_+ + k_e + k_r) e^{\lambda_+ t} - (\lambda_- + k_e + k_r) e^{\lambda_- t} \right), \quad (20)$$

$$c_s \approx \left(\frac{k_a L_0}{\lambda_+ - \lambda_-} \right) (e^{\lambda_+ t} - e^{\lambda_- t}), \quad (21)$$

$$c_i \approx k_e e^{-k_{deg} t} \int_0^t c_s e^{k_{deg} s} ds = \left(\frac{k_e k_a L_0}{\lambda_+ - \lambda_-} \right) \left(\frac{e^{\lambda_+ t} - e^{-k_{deg} t}}{k_{deg} + \lambda_+} - \frac{e^{\lambda_- t} - e^{-k_{deg} t}}{k_{deg} + \lambda_-} \right), \quad (22)$$

$$r_s \approx \left(\frac{k_a L_0}{\lambda_+ - \lambda_-} \right) \left(\left(\frac{\lambda_- + k_e}{\lambda_- + k_t} \right) (e^{\lambda_- t} - e^{-k_t t}) - \left(\frac{\lambda_+ + k_e}{\lambda_+ + k_t} \right) (e^{\lambda_+ t} - e^{-k_t t}) \right), \quad (23)$$

$$r_i = k_t \int_0^t r_s e^{k_{deg}(s-t)} ds, \quad (24)$$

where λ_{\pm} are the roots of the quadratic equation

$$\lambda^2 + (k_a + k_r + k_e)\lambda + k_a k_e = 0. \quad (25)$$

Figs. 3 and 4 illustrate the quality of the approximations for two cases that differ only in the recycling fractions. Fig. 3 considers the parameter values shown in Table 1 except for $f_1 = f_2 = 1.0$ and consequently Eq. (6b,c) implies that $R_{s0} = 4,333$ and $R_{i0} = 59,091$. Since δ is inversely proportional to the cell concentration the cases $n = 1.0 \times 10^9$ and 1.0×10^{10} cells/l correspond to $\delta = 137$ and 13.7, respectively. In both cases the approximation is very good for short times, but begins to deteriorate after C_s attains its maximum. In light of the high δ values considered in Fig. 3, the approximations are surprisingly good. Fig. 4 considers a similar case, but with recycling (the parameter values shown in Table 1 except for $f_1 = 1.0$). In this case the cell concentrations $n = 1.0 \times 10^9$ and $n = 1.0 \times 10^{10}$ cells/l correspond to $\delta = 5.0$ and 0.5, respectively. Eqs. (20)–(22) are very good approximations during the surface binding phase for both cell concentrations, however, in the low-density case ($\delta = 5.0$) the quality of the approximation eventually deteriorates due

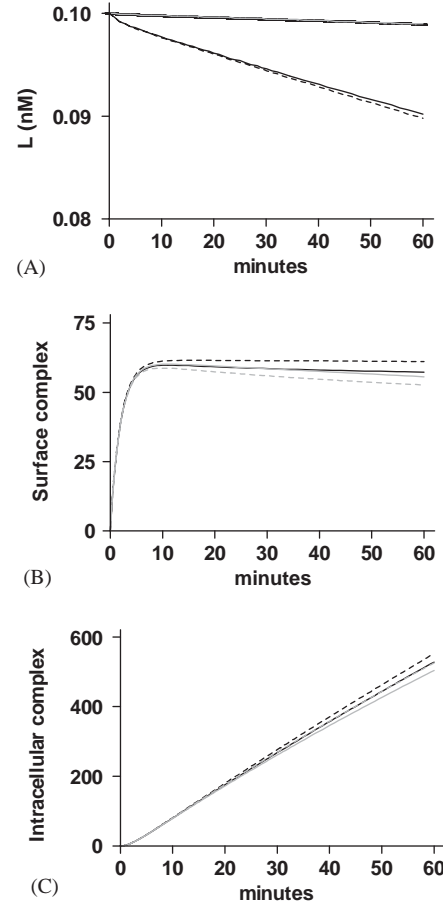


Fig. 3. (A–C) Protocol I in the absence of recycling. Approximations (20)–(22) (dashes) versus numerical solution of Eqs. (1)–(3) (solid lines) for $L_0 = 0.1$ nM and the parameter values listed in Table 1, except $f_1 = f_2 = 1$ ($R_{s0} = 4,333$, $R_{i0} = 59,091$). Color scheme: (gray) $n = 1.0 \times 10^9$ cell/l, $\delta = 137$ (black) $n = 1.0 \times 10^{10}$ cell/l, $\delta = 13.7$.

to the deviation of R_s from its initial value (not shown). Nevertheless, the overall fit is still very good for $\delta = 5.0$, which stems from the fact that the importance of the $k_f LR_s$ term in Eqs. (1), (2) and (4) diminishes as the extracellular ligand concentration decreases with time. Thus, the approximations derived in this section under the assumption that $\delta \ll 1$, seem to be of a much wider validity. Eqs. (20)–(22) were obtained by neglecting recycling effects. Nevertheless, these equations are better approximations for the case considered in Fig. 4, which does include recycling. Thus, at least for the parameter values considered in Table 1 ligand kinetics depend more strongly on δ than on the kinetics of the free (surface and internalized) receptors.

3.2. Protocol II

Instead of solving Eqs. (1)–(5), we shall consider the initial transient approximation (ITA) of these equations. The latter is derived by noting that at sufficiently short times initial conditions (7) imply that all terms proportional to L can be safely neglected so that the system is

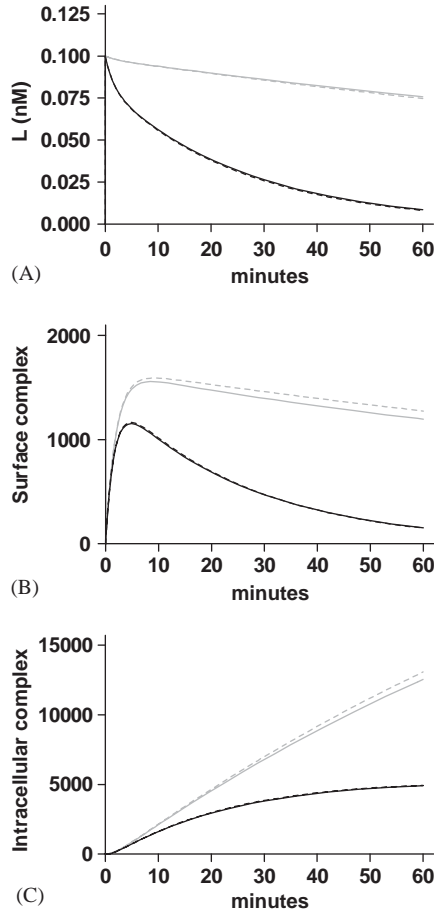


Fig. 4. (A–C) Protocol I in the presence of recycling. Approximations (20)–(22) (dashes) versus numerical solution of Eqs. (1)–(3) (solid lines) for $L_0=0.1$ nM and the parameter values listed in Table 1, except $f_1 = 1$ ($R_{s0} = 118, 575$, $R_{j0} = 118, 182$). Color scheme: (gray) $n = 1.0 \times 10^9$ cell/l, $\delta = 5.0$ (black) $n = 1.0 \times 10^{10}$ cell/l, $\delta = 0.5$.

Table 1
Base line parameter values

Parameter	Process	Value
k_r	Ligand desorption	0.34 min^{-1}
k_f	Ligand adsorption	$7.2 \times 10^7 \text{ M}^{-1} \text{ min}^{-1}$
k_t	Constitutive internalization	0.030 min^{-1}
k_e	Endocytosis	0.165 min^{-1}
k_{deg}	Receptor degradation	0.0022 min^{-1}
k_{rec}	Receptor recycling	0.058 min^{-1}
V_r	Receptor synthesis	$130 \text{ receptors/cell min}^{-1}$
f_1	Endosomal sorting	0.5
f_2	Endosomal sorting	0.5

Parameter values are average estimates from Lauffenburger and Linderman (1993, p. 95). Substituting these values into Eq. (6) yields $R_{s0} = 118, 575$ and $R_{j0} = 118, 182$.

well approximated by the following *linear* system:

$$\dot{L} \approx (k_r C_s)(n/N_{av}), \quad (26)$$

$$\dot{C}_i \approx -(k_r + k_e)C_s + (1 - f_1)k_{rec}C_i, \quad (27)$$

$$\dot{C}_i = k_e C_s - ((1 - f_1)k_{rec} + f_1 k_{deg})C_i, \quad (28)$$

$$\dot{R}_s \approx k_r C_s + V_r - k_t R_s + (1 - f_2)k_{rec}R_i, \quad (29)$$

$$\dot{R}_i = k_t R_s - ((1 - f_2)k_{rec} + f_2 k_{deg})R_i. \quad (30)$$

Inspection of Eq. (1) reveals that a sufficient condition for the validity of this approximation is

$$k_f L R_s \ll k_r C_s \Rightarrow K_D C_s / R_s \gg L, \quad (31)$$

where $K_D = k_r/k_f$ is the ligand-surface receptor binding affinity. On the other hand, initial conditions (7) imply that in protocol II all the free extracellular ligand is due to the dissociation of surface complex and consequently,

$$L \leq C_{s2}(n/N_{av}). \quad (32)$$

Combining Eqs. (31) and (32) we obtain the following sufficient condition for the validity of the approximation up to time t

$$C_s(t)/C_{s2} \gg (R_{s0}/K_D)(n/N_{av}). \quad (33)$$

Noting that Eqs. (27) and (28) are an autonomous linear system we obtain

$$C_s \approx \frac{C_{s2}}{p_+ - p_-} ((p_+ + K_1)e^{p_+ t} - (p_- + K_1)e^{p_- t}), \quad (34)$$

$$C_i \approx \frac{k_e C_{s2}}{p_+ - p_-} (e^{p_+ t} - e^{p_- t}), \quad (35)$$

where p_{\pm} are the roots of the quadratic equation

$$p^2 + (K_1 + k_r + k_e)p + k_r K_1 + f_1 k_{deg} k_e = 0 \quad (36)$$

and

$$K_1 \equiv (1 - f_1)k_{rec} + f_1 k_{deg}. \quad (37)$$

Using results (34) and (35) one can proceed to integrate Eqs. (26), (29) and (30).

Fig. 5 illustrates the quality of the approximations for two cell concentrations, $n = 1.0 \times 10^8$ and $n = 1.0 \times 10^9$ cells/l. As can be seen, results (34) and (35) are the low cell concentration limits implied by Eqs. (2) and (3). In fact, for the cell concentration $n = 1.0 \times 10^7$ cells/l, numerical solutions are indistinguishable from the corresponding approximations (not shown). Moreover, whereas C_s decreases significantly before cell concentration effects become apparent, the dependence of C_i on cell concentration is rather pronounced. This behavior is consistent with Eq. (33), which implies that the approximation leading to Eqs. (34) and (35) will begin to break down as the number of surface-bound ligand molecules decreases below a threshold level that scales linearly with the cell concentration, n .

3.2.1. Non-recycling receptors

In the case of non-recycling receptors, $f_1 = 1$, so that $p_+ = -k_{deg}$ and $p_- = -(k_e + k_r)$. Thus, for non-recycling receptors Eqs. (34) and (35) take on the simple

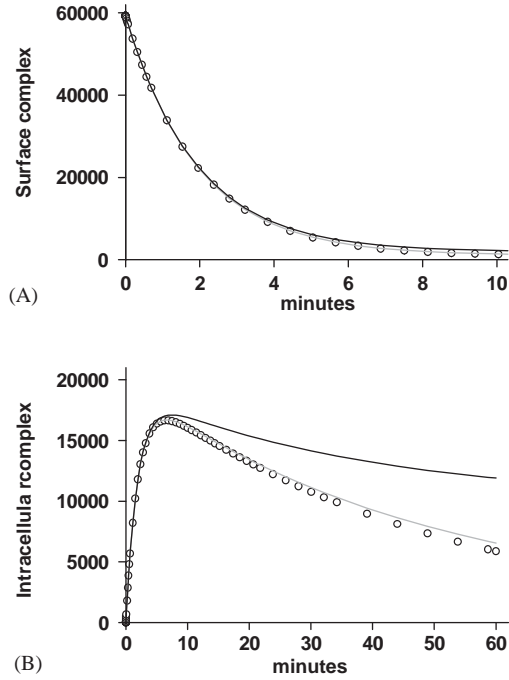


Fig. 5. (A, B) By protocol II: Approximations (34) and (35) (circles) versus numerical solution of Eqs. (2) and (3) (solid lines) using the parameter values listed in Table 1 and the initial conditions $C_{s2} = R_{s2} = 0.5R_{s0}$. Color scheme: (black) $n = 1.0 \times 10^9$ cell/l, (gray) $n = 1.0 \times 10^8$ cell/l.

form

$$C_s \approx C_{s2} e^{-(k_r + k_e)t}, \quad (38)$$

$$C_i \approx \frac{k_e C_{s2}}{k_r + k_e - k_{deg}} (e^{-k_{deg}t} - e^{-(k_r + k_e)t}). \quad (39)$$

These results were previously derived by Shimizu and Kawashima (1989). However, these authors did not consider the case of recycling receptors, nor did they derive a criterion for the validity of their approximation.

3.3. Protocol III

Anticipating that the free extracellular ligand concentration is negligible we consider Eqs. (26)–(30) once more. Solving the autonomous pair (27)–(28) subject to initial conditions (8) we obtain

$$C_i \approx \frac{C_{i3}}{p_+ - p_-} ((p_+ + k_e + k_r)e^{p_+t} - (p_- + k_e + k_r)e^{p_-t}), \quad (40)$$

$$C_s \approx \frac{(1 - f_1)k_{rec}C_{i3}}{p_+ - p_-} (e^{p_+t} - e^{p_-t}), \quad (41)$$

where p_{\pm} are defined by Eq. (36). In contrast to protocol II C_i is non-zero initially. Consequently, Eq. (31) is no longer the sole criterion for neglecting the extracellular ligand concentration in Eqs. (2) and (3) and must be

augmented by an additional requirement that

$$k_f LR_s \ll (1 - f_1)k_{rec}C_i, \quad (42)$$

since this ensures that the term $k_f LR_{s0}$ can be neglected in Eq. (2). On the other hand, initial conditions (8) imply that

$$L \leq C_{i3}(n/N_{av}). \quad (43)$$

Consequently, the criterion for the validity of the approximation up to time t is

$$\frac{C_i(t)}{C_{i3}} \gg \frac{R_{s0}(n/N_{av})}{k_{rec}(1 - f_1)/k_f}. \quad (44)$$

Fig. 6 illustrates the quality of the approximations for two cell concentrations, $n = 1.0 \times 10^8 - 1.0 \times 10^9$ cells/l. As can be seen, results (40) and (41) are the low cell concentration limits implied by Eqs. (2) and (3). In fact, for a cell concentration of $n = 1.0 \times 10^7$ cells/l the numerical solutions are indistinguishable from the approximations (not shown). Moreover, whereas C_i decreases significantly before cell concentration effects become apparent, the dependence of C_s on cell concentration is rather pronounced. This behavior is consistent with Eq. (44), which implies that the approximation leading to Eqs. (40) and (41) will begin to break down as the number of intracellular ligand molecules

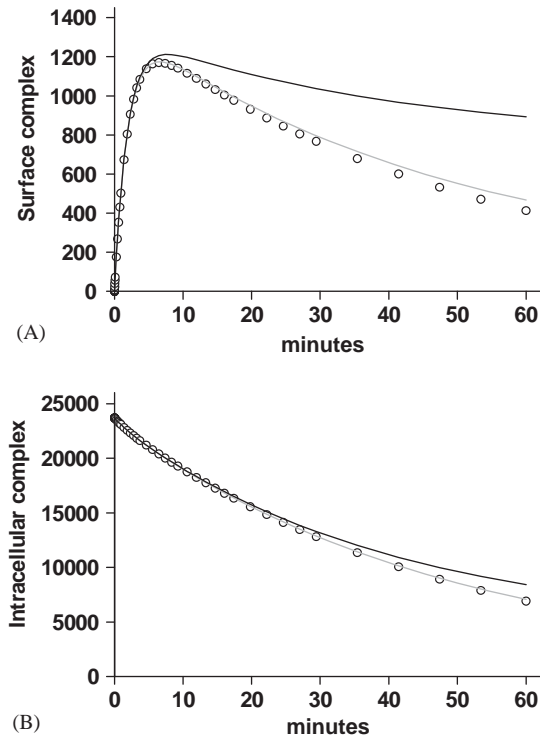


Fig. 6. (A, B) Protocol III. Approximations (40) and (41) (circles) versus numerical solution of Eqs. (2) and (3) (solid lines) using the parameter values listed in Table 1 and the initial conditions $R_{s3} = R_{s0}$, $C_{i3} = 0.2R_{s0}$. Color scheme: (black) $n = 1.0 \times 10^9$ cell/l, (gray) $n = 1.0 \times 10^8$ cell/l.

decreases below a threshold level that scales linearly with the cell concentration, n .

In a series of studies Maxfield and co-workers used protocol III to follow the total number of cell-associated ligand molecules (Dunn et al., 1989; Ghosh et al., 1994; Hao and Maxfield, 2000). Summing Eqs. (40) and (41) yields the following simple approximation for the latter quantity:

$$C_s + C_i \approx \frac{C_{i3}}{p_+ - p_-} ((p_+ + k_e + k_r + \bar{k}_{rec})e^{p_+ t} - (p_- + k_e + k_r + \bar{k}_{rec})e^{p_- t}), \quad (45a)$$

where we introduced the simplifying notation

$$\bar{k}_{rec} = (1 - f_1)k_{rec}. \quad (45b)$$

Hao and Maxfield (2000) used protocol III to study the kinetics of the fluorescent lipid marker C₆-NBD-SM in CHO cells and fit their experimental results to a double exponential decay with a *non-zero* plateau. Since they introduced this approximation in an ad hoc manner, they were unable to directly correlate between their fitting parameters and the kinetic process, as is done in Eqs. (40) and (41). Moreover, their assumption of a non-zero plateau is inconsistent with Eq. (45a), and indeed with the base model itself since the latter is a network with an irreversible sink. Thus, the experiments of Hao and Maxfield (2000) could imply that internalized C₆-NBD-SM is sequestered in CHO cells. Alternatively, saturation of the post-endocytotic trafficking (French et al., 1994) may result in a very low degradation rate and consequently in an apparent plateau.

3.3.1. Non-recycling receptors

In the case of non-recycling receptors $f_1 = 1, p_+ = -k_{deg}$ and $p_- = -(k_e + k_r)$, so that Eqs. (40) and (41) take on the simple form

$$C_i \approx C_{i3}e^{-k_{deg}t}, \quad (46)$$

$$C_s \approx 0. \quad (47)$$

Thus, negligible numbers of surface complexes in protocol III directly imply that the cells are non-recycling. Furthermore, these results imply that for non-recycling receptors the total number of cell-associated ligand molecules decays exponentially.

3.3.2. Fast recycling and endocytosis

As we shall proceed to demonstrate, the total number of cell-associated ligand molecules also decays exponentially whenever endocytosis and or recycling are fast compared to ligand desorption from surface receptors and intracellular degradation of internalized ligand-receptor complexes,

$$k_r + f_1 k_{deg} \ll \bar{k}_{rec} + k_e. \quad (48a)$$

To see this, we note that the latter inequality implies that $k_r K_1 + f_1 k_{deg} k_e \ll (K_1 + k_e + k_r)^2$. (48b)

Recalling that p_{\pm} are the roots of Eq. (36) we have

$$p_{\pm} = \frac{(K_1 + k_r + k_e)}{2} \left(1 \pm \sqrt{1 - \frac{4(k_r K_1 + f_1 k_{deg} k_e)}{(K_1 + k_r + k_e)^2}} \right). \quad (49)$$

Consequently, inequality (48a) implies that we can use the binomial expansion of the square root in Eq. (49), $\sqrt{1 - x} \approx 1 - x/2$, to obtain the following approximations:

$$p_+ \approx -\frac{k_r K_1 + f_1 k_{deg} k_e}{K_1 + k_e + k_r} \approx -\frac{k_r \bar{k}_{rec} + f_1 k_{deg} k_e}{\bar{k}_{rec} + k_e}, \quad (50a)$$

$$p_- \approx -(K_1 + k_e + k_r) \approx -(\bar{k}_{rec} + k_e + k_r). \quad (50b)$$

Moreover, Eq. (48b) implies that $p_+/p_- \ll 1$. Substituting Eqs. (50a,b) into Eq. (45a) we arrive at the final result

$$\frac{C_s + C_i}{C_{i3}} \approx \left(\frac{p_+ + k_e + k_r + \bar{k}_{rec}}{p_+ - p_-} \right) e^{p_+ t} \approx e^{p_+ t}, \quad (51)$$

where p_+ is given by Eq. (50a).

Taken together, the results of the last two subsections imply that a monoexponential decay of the total number of cell-associated ligands is not a unique hallmark of a single process. In the case of non-recycling receptors, this apparent rate constant corresponds to the degradation rate constant k_{deg} , whereas in the case of slow degradation and desorption it corresponds to an effective recycling rate constant defined in Eq. (50a). Inequalities (48a) and (48b) imply that the latter is much smaller than the true recycling rate constant, k_{rec} . The practice of estimating the recycling rate constant as the monoexponential decay constant in protocol III (Ghosh et al., 1994) can therefore lead to significant errors.

4. Parameter estimation and model validation

Each of the approximate solutions derived in the previous section was found to depend on different subsets of model parameters. Obviously, protocols I–III are only sensitive to parameters appearing in the corresponding approximations. Whenever this dependence is explicit, not only is the protocol sensitive to the parameter, it also provides a direct and unambiguous way of estimating the parameter. As we shall now argue, combining the different protocols results in improved parameter estimation.

As reviewed by Lauffenburger and Linderman (1993) the binding parameters, R_{s0} , k_f , and k_r can be estimated from ligand-binding experiments at low temperatures such that endocytosis is inhibited. Such an a priori estimate is important for designing protocol I

experiments under excess receptor conditions as defined by Eq. (11). In the latter case Eqs. (20)–(25) can be used to study slowly recycling receptors. The structure of Eqs. (20) and (21) implies that λ_{\pm} can be estimated directly as the exponential decay rates. Consequently, fitting the extracellular ligand concentration to Eq. (20) yields a direct estimate of $k_e + k_r$, whereas fitting the concentration of surface-bound ligand to Eq. (21) yields a direct estimate of $k_f R_{s0}$ (k_a). Noting that Eq. (25) implies that $\lambda_+ \lambda_- = k_a k_e$ we can combine the estimates of k_a , λ_+ , λ_- , $k_e + k_r$ to obtain an indirect estimate of $k_e = \lambda_+ \lambda_- / k_a$ and k_r . Thus, protocol I can be used under excess receptor conditions to sequentially estimate the extracellular parameters $k_f R_{s0}$, k_r and k_e for slowly recycling receptors.

In order to estimate intracellular parameters of the base model one has to resort to protocols II and III. Thus, our analysis of protocol II implies that whenever the base model is valid, fitting the concentration of surface-bound ligand to Eq. (34) yields a direct estimate of $K_1 \equiv (1 - f_1)k_{rec} + f_1 k_{deg}$, whereas fitting the concentration of internalized ligand to Eq. (35) yields a direct estimate of k_e . Similarly, our analysis of protocol III implies that whenever the base model is valid, fitting the concentration of internalized ligand to Eq. (40) yields a direct estimate of $k_r + k_e$, whereas fitting the concentration of surface-bound ligand to Eq. (41) yields a direct estimate of $(1 - f_1)k_{rec}$. Combining these estimates with the estimate of K_1 and k_e by protocol II yields an indirect estimate of $f_1 k_{deg}$ and k_r . Moreover, the fact that $k_r + k_e$ is directly estimated by protocols I and III allows a self-consistency check of the model.

The simple relationships between rate constants and ligand numbers implied by Eqs. (35) and (41) not only suggest a simple means of estimating k_e and $\bar{k}_{rec} \equiv (1 - f_1)k_{rec}$, but are also definitive predictions that are useful for *model validation*. Furthermore, the finding that the apparent rate constants for protocols II and III are the same, but different from the rate constants of the same system under protocol I is a definitive result that can be used to assess the model's validity for a given biological system. The most striking manifestation of this result is obtained by dividing Eq. (35) by Eq. (41) to find

$$\frac{(C_{i,II}/C_{s2})}{(C_{s,III}/C_{i3})} \approx \frac{k_e}{\bar{k}_{rec}}, \quad (52)$$

where the subscripts II and III denote the corresponding experimental protocol. Namely, our analysis predicts that at the low cell concentration limit, the ratio of the number of internalized ligand molecules measured with protocol II to the number of surface-bound ligand molecules measured for protocol III is approximately *constant*. Fig. 7 illustrates the validity of this prediction for the baseline parameters listed in Table 1. Different pre-loading conditions such as temperature of the

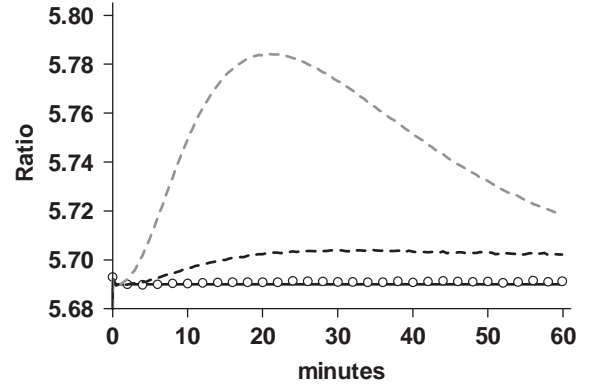


Fig. 7. Dual-protocol In/Sur plot. The ratio of internalized ligand–receptor complexes in protocol II to surface ligand–receptor complexes in protocol III, $C_{i,II}/C_{s,III}$, as a function of cell concentration is plotted against time. Numerical simulations are shown for $n = 1.0 \times 10^9$ cell/l (gray dashes), $n = 1.0 \times 10^8$ cell/l (black dashes) and $n = 1.0 \times 10^7$ cell/l (circles). The latter is well approximated by the constant value predicted by Eq. (52) (solid black). These results were obtained using the parameter values listed in Table 1 and the initial conditions $R_{s2} = R_{s3} = R_{s0}$, $C_{i2} = C_{i3} = 0.5R_{s0}$.

binding medium and duration of the loading phase will result in different values of C_{s2} and C_{i3} . Since k_e and $\bar{k}_{rec} \equiv (1 - f_1)k_{rec}$ may vary with media conditions, care should be taken in applying Eq. (52) only to data pooled from protocols II and III that were conducted in similar media conditions (temperature, pH, etc.).

5. Discussion

The current analysis of the base model of endocytosis and receptor recycling has yielded several unexpected results that are hard to obtain by exhaustive simulation. The finding that for protocol I the system responds linearly over a very wide range of ligand concentrations was obtained by neglecting the variation in the number of free surface receptors in Eqs. (1) and (2) and therefore implies that ligand kinetics are effectively *decoupled* from receptor kinetics in these cases. Thus, ligand kinetics depend on free receptor recycling only *implicitly* since the latter determines the number of free surface-receptors at homeostasis as in Eq. (6b,c), thereby affecting k_a (see Eq. (17)). The analysis of protocols II–III yielded the striking prediction that the ratio of the number of internalized ligand molecules measured with protocol II to the number of surface-bound ligand molecules measured for protocol III is approximately *constant*. Such definitive predictions are potentially useful for model validation. The need for better methods of model validation and parameter estimation is illustrated by the recent finding that direct measurements of receptor recycling could yield much higher recycling rates than previously estimated (Hao and Maxfield, 2000). Our analysis of protocol III

suggests that this discrepancy stems from the fact that fast endocytosis and fast recycling may be wrongly interpreted by graphical methods as slow *apparent* endocytosis and slow *apparent* recycling.

An attractive feature of the present analysis is that it provides direct and transparent information on the sensitivity of three accepted protocols to the various model parameters. The alternative of obtaining this information from a numerical sensitivity analysis is less informative as it is restricted to a narrow region of parameter space (Waters et al., 1990). Moreover, numerical sensitivity analysis does not explain why a given experimental protocol is sensitive to certain parameters while insensitive to others. Such information is inherent to the derivation of our approximations and is transparent in the final approximations. Knowing the sensitivity of a given protocol to different model parameters is important not only for parameter estimation, but also for mechanism identification. Thus, for example, the recent controversy regarding the role of dynamin in ligand-induced endocytosis was the result of using an inconclusive protocol to pin down a mechanism. Namely, Damke et al. (1994) measured the concentration of internalized EGF in protocol I experiments with cells that expressed wild type dynamin and mutant dynamin. They observed that internalization was down regulated in cells that over express the mutant dynamin and inferred from this that endocytosis is down regulated by mutant dynamin. However, Ringerike et al. (1998) recently found that over expression of mutant dynamin results in reduced EGF binding onto EGF receptors and postulated that this could explain the findings of Damke et al. (1994). That both effects can explain the observed down regulation in ligand internalization is clearly seen in Eq. (22), since according to this result internalized ligand concentration is proportional to the product $(k_f R_{s0})k_e$. However, our analysis goes beyond just demonstrating the source of this controversy. In fact, it points to a possible resolution. That is, our analysis of protocol II yielded Eq. (35), which implies that the concentration of internalized ligand is proportional only to k_e . In turn, this implies that protocol II is highly sensitive to variations in the endocytosis rate constant.

Protocols I–III are not directly sensitive to the degradation rate constant, k_{deg} . However, the combined analysis of protocols II and III provided a simple in situ method for estimating k_{deg} . The prevailing approach of estimating k_{deg} from the kinetics of extracellular degradation products is restrictive and may lead to wrong interpretations regarding the time lag that is often associated with intracellular degradation (Lauffenburger and Linderman, 1993). This is important not only for improving the estimate of the intracellular degradation rate constant, but also for validating the modeling of intracellular degradation. For example,

Mullick and Katzenellenbogen (1986) showed that the lag time in the regulation of progesterone receptor profile could be explained by a new kinetic model that included a “precursor step” before the degradation of progesterone receptor.

Our analysis of the base model is easily extended to include first-order extracellular degradation of ligand in Eq. (1). Moreover, an inclusion of a ligand-induced receptor synthesis term of the form $k_{syn}C_s$ in Eq. (4) (Fallon and Lauffenburger, 2000) would not affect our analysis at all. Such a nonlinear term would not affect the linear stability analysis of protocol I. Similarly, our analysis of protocols II and III was based on a decoupling of ligand kinetics from free receptor kinetics and would consequently be unaffected. Thus, ligand-induced receptor synthesis does not significantly alter ligand kinetics and its existence can only be validated by a closer analysis of free receptor kinetics.

However, the analysis of protocols II and III relies heavily on the assumption of first order kinetics underlying the base model. Namely, neglectation of extracellular ligand concentration in Eqs. (2) and (4) renders these equations linear, thereby allowing the derivation of simple bi-exponential approximations. This approach can also be used to analyse the base model’s response to a variant of protocol III in which the surface-bound ligand is not removed prior to the temperature jump (Wang et al., 2002). However, this also implies that our analysis of protocols II and III will not be applicable whenever the assumption of non-saturable first-order mass transfer kinetics between intracellular compartments breaks down. As already mentioned, the apparent plateau in intracellular ligand concentration observed by Hao and Maxfield (2000) cannot be explained by the base model and may require the inclusion of a saturable post-endocytotic trafficking term as proposed by French et al. (1994).

The base model is only relevant for ligands, which like EGF remain associated with their receptors during sorting (Lauffenburger and Linderman, 1993). However, dissociation of the receptor–ligand complex is pH dependent for certain ligands, such as TGF (Ebner and Derynck, 1991; French et al., 1995). To capture this effect the base model must be augmented by a compartment of free intracellular ligand that can reversibly bind to intracellular receptors, the addition of a mass balance equation for the concentration of free intracellular ligand, L_i , and of terms in Eqs. (3)–(5) to describe binding and dissociation of the form $k_f R_i L_i$ and $k'_r C_i$, respectively (Starbuck and Lauffenburger, 1992). This does not affect the leading order approximations of protocol I that lead to Eq. (9), nor results (12) and (13) obtained for protocol I on cells without receptor recycling. According to Starbuck and Lauffenburger (1992) the pH drop between the extracellular and endosomal compartments can result in a 10-fold

increase in the binding off-rate of the ligand–receptor complex, (e.g., $k'_r = 10k_r$). Such pH effects will lower the number of intracellular complexes per cell predicted by the base model for protocols I–II since both these protocols start with no intracellular complex. In the absence of recycling, pH effects will not affect the base model prediction of the number of surface complexes per cell, Eq. (38). For cells with receptor recycling, pH effects result in an overestimation of complex recycling by the base model and a corresponding overestimation of the number of surface complexes per cell and the concentration of free extracellular ligand. Protocol III should be the most sensitive to pH effects as in this case a sizable fraction of the pre-loaded drug is free and the pool of pre-loaded intracellular complex is relatively short-lived because of the high binding off-rate. Consequently, the base model overestimates the numbers of surface and intracellular complexes. Thus, pH effects can lead to significant deviations from the base model estimates of $C_{i,II}$ and $C_{s,III}$ and to the consequent invalidation of result (52). This is but one example of the usefulness of internal-consistency checks such as Eq. (52) in validating or refuting a model.

Acknowledgements

The authors wish to thank Dr. Matthew Walker III for careful reading of the manuscript and Mrs. Alisa Tzafiriri for the preparation of Fig. 1. This study was supported in part by grants from the National Institutes of Health (HL60407, HL62457 and HL49309) and an External Research Program Postdoctoral Fellowship (ART) from Philip Morris USA Inc.

Appendix A. Linear stability analysis

Setting the right-hand sides of Eqs. (1)–(5) to zero we find that as long as $f_1 k_{deg} > 0$ the base model has a single-steady state

$$(L, R_s, C_s, C_i, R_i) = (0, R_{s0}, 0, 0, R_{i0}), \quad (\text{A.1})$$

where R_{s0} and R_{i0} are both defined in Eq. (6). Introducing the simplifying notations

$$k_a = k_f R_{s0} (n/N_{av}), \quad (\text{A.2})$$

$$c_s = C_s (n/N_{av}), \quad c_i = C_i (n/N_{av}),$$

$$r_s = (R_s - R_{s0}) (n/N_{av}), \quad r_i = (R_i - R_{i0}) (n/N_{av}) \quad (\text{A.3})$$

and linearizing the system around this steady-state we find

$$\dot{L} = (-k_a L + k_r c_s), \quad (\text{A.4})$$

$$\dot{c}_s = k_a L - (k_r + k_e) c_s + (1 - f_1) k_{rec} c_i, \quad (\text{A.5})$$

$$\dot{c}_i = k_e c_s - ((1 - f_1) k_{rec} + f_1 k_{deg}) c_i, \quad (\text{A.6})$$

$$\dot{r}_s = -k_a L + k_r c_s - k_i r_s + (1 - f_2) k_{rec} r_i, \quad (\text{A.7})$$

$$\dot{r}_i = k_i r_s - ((1 - f_2) k_{rec} + f_2 k_{deg}) r_i. \quad (\text{A.8})$$

Note that this set of five linear equations partitions into two autonomous sets, the first three equations describing the relaxation of the ligand concentration in the vicinity of the steady state and the last two linearized equations describing the relaxation of free receptor number in the vicinity of the steady state. Rewriting Eqs. (A.4)–(A.8) in matrix form

$$\begin{pmatrix} \dot{L} \\ \dot{c}_s \\ \dot{c}_i \end{pmatrix} = \begin{pmatrix} -k_a & k_r & 0 \\ k_a & -(k_r + k_e) & (1 - f_1) k_{rec} \\ 0 & k_e & -((1 - f_1) k_{rec} + f_1 k_{deg}) \end{pmatrix} \times \begin{pmatrix} L \\ c_s \\ c_i \end{pmatrix}, \quad (\text{A.9})$$

it is easy to verify that the determinant of the matrix is $-k_a k_e f_1 k_{deg}$. Consequently, the determinant is negative whenever $f_1 k_{deg} > 0$. Noting that the determinant is equal to the product of the eigenvalues and that the trace of the matrix is also negative, we conclude that the real parts of all three eigenvalues are negative and consequently, that the steady-state point is linearly stable. The vanishing of the determinant for $f_1 k_{deg} = 0$ ($f_1 = 0$) is a reflection of the fact that in this case total ligand concentration is conserved, so that

$$c_i = L_0 - L - c_s, \quad f_1 = 0. \quad (\text{A.10})$$

Appendix B. Leading order approximations for protocol I

Although Eqs. (1)–(6) cannot be solved in closed form they can be approximated using the method of successive substitutions (Lin and Segel, 1988; Hill, 1942). This iterative process of approximation begins by using the initial conditions as the lowest order approximations, which are then used to obtain first-order approximations and so on. Using subscripts to denote the order of the approximation (iteration) we find the following equations for the first-order approximations:

$$\dot{L}_1 = (-k_f L_0 R_{s0}) (n/N_{av}), \quad (\text{B.1})$$

$$\dot{C}_{s1} = k_f L_0 R_{s0}, \quad (\text{B.2})$$

$$\dot{C}_{i1} = 0, \quad (\text{B.3})$$

$$\begin{aligned}\dot{R}_{s1} &= -k_f L_0 R_{s0} + V_r - k_t R_{s0} + (1 - f_2)k_{rec} R_{i0} \\ &= -k_f L_0 R_{s0},\end{aligned}\quad (\text{B.4})$$

$$\dot{R}_{i1} = k_t R_{s0} - ((1 - f_2)k_{rec} + f_2 k_{deg}) R_{i0} = 0. \quad (\text{B.5})$$

Integrating these equations subject to initial conditions (6) we find

$$L_1 = L_0 - k_a t, \quad (\text{B.6})$$

$$C_{s1} = (k_f L_0 R_{s0}) t, \quad (\text{B.7})$$

$$C_{i1} = 0, \quad (\text{B.8})$$

$$R_{s1} = R_{s0} - (k_f L_0 R_{s0}) t, \quad (\text{B.9})$$

$$R_{i1} = R_{i0}. \quad (\text{B.10})$$

The next order of the approximation is defined by the following system of equations:

$$\dot{L}_2 = (-k_f L_1 R_{s1} + k_r C_{s1})(n/N_{av}), \quad (\text{B.11})$$

$$\dot{C}_{s2} = k_f L_1 R_{s1} - (k_r + k_e) C_{s1}, \quad (\text{B.12})$$

$$\dot{C}_{i2} = k_e C_{s1} = k_e (k_f L_0 R_{s0}) t, \quad (\text{B.13})$$

$$\begin{aligned}\dot{R}_{s2} &= -k_f L_1 R_{s1} + k_r C_{s1} + V_r - k_t R_{s1} \\ &\quad + (1 - f_2)k_{rec} R_{i1},\end{aligned}\quad (\text{B.14})$$

$$\begin{aligned}\dot{R}_{i2} &= (k_t R_{s0} - ((1 - f_2)k_{rec} + f_2 k_{deg}) R_{i0}) \\ &\quad - k_t (k_f L_0 R_{s0}) t = -k_t (k_f L_0 R_{s0}) t.\end{aligned}\quad (\text{B.15})$$

Substituting the first-order approximation on the right-hand sides of Eqs. (B.11)–(B.15) and integrating these equations subject to initial conditions (6) we find

$$L_2 = L_1 + \frac{1}{2} k_a (k_f L_0 + k_a + k_r) t^2 - \frac{1}{3} k_f k_a^2 t^3, \quad (\text{B.16})$$

$$\begin{aligned}C_{s2} &= C_{s1} - \frac{1}{2} k_f R_{s0} (L_0 (k_r + k_e) + k_a + k_f L_0^2) t^2 \\ &\quad + \frac{1}{3} k_f (k_f L_0 R_{s0}) k_a t^3,\end{aligned}\quad (\text{B.17})$$

$$C_{i2} = \frac{1}{2} k_e (k_f L_0 R_{s0}) t^2, \quad (\text{B.18})$$

$$\begin{aligned}R_{s2} &= R_{s1} + \frac{1}{2} k_f R_{s0} (k_a + k_f L_0^2 + L_0 (k_t + k_r)) t^2 \\ &\quad - \frac{1}{3} k_f (k_f L_0 R_{s0}) k_a t^3,\end{aligned}\quad (\text{B.19})$$

$$R_{i2} = R_{i0} - \frac{1}{2} k_t (k_f L_0 R_{s0}) t^2. \quad (\text{B.20})$$

Clearly, this iterative procedure yields the leading terms in the Taylor expansion of all the variables. Two results are of special interest. First, we note that V_r does not appear explicitly in these approximations, nor will it appear in higher order terms since it cancels out in the first order term. Second, Eqs. (B.7), (B.17) and (B.18) imply that

$$\begin{aligned}\frac{C_i}{C_s} &= \left(\frac{k_e}{2}\right) t + \frac{1}{4} k_e (k_r + k_e + k_f R_{s0} (n/N_{av})) \\ &\quad + k_f L_0 t^2 + O(t^3).\end{aligned}\quad (\text{B.21})$$

References

- Bajzer, Z., Myers, A.C., Kovach, J.S., Vuk-Pavlovic, S., 1989. Binding, internalization, and intracellular processing of proteins interacting with recycling receptors. *J. Biol. Chem.* 264, 13623–13631.
- Buchman, E., Parnas, H., 1994. Sequential approach for describing channel opening and desensitization. *J. Theor. Biol.* 167, 381–395.
- Damke, H., Baba, T., Warnock, D.E., Schmid, S.L., 1994. Induction of mutant dynamin specifically blocks endocytic coated vesicle formation. *J. Cell. Biol.* 127, 915–934.
- Dunn, K.W., McGraw, T.E., Maxfield, F.R., 1989. Iterative fractionation of recycling receptors from lysosomally destined ligands in an early sorting endosome. *J. Cell. Biol.* 109, 3303–3314.
- Ebner, R., Derynck, R., 1991. Epidermal growth factor and transforming growth factor alpha: differential intracellular routing and processing of ligand–receptor complexes. *Cell Regul.* 2, 599–612.
- Fallon, E.M., Lauffenburger, D.A., 2000. Computational model for effects of ligand/receptor binding properties on interleukin-2 trafficking dynamics and T cell proliferation response. *Biotechnol. Prog.* 16, 905–916.
- Fannon, M., Nugent, M.A., 1996. Basic fibroblast growth factor binds its receptors, is internalized, and stimulates DNA synthesis in Balb/c3T3 cells in the absence of heparan sulfate. *J. Biol. Chem.* 271, 17949–17956.
- French, A.R., Sudlow, G.P., Wiley, H.S., Lauffenburger, D.A., 1994. Postendocytic trafficking of epidermal growth factor–receptor complexes is mediated through saturable and specific endosomal interactions. *J. Biol. Chem.* 269, 15749–15755.
- French, A.R., Tadaki, D.K., Niyogi, S.K., Lauffenburger, D.A., 1995. Intracellular trafficking of epidermal growth factor family ligands is directly by the pH sensitivity of the receptor/ligand interaction. *J. Biol. Chem.* 270, 4334–4340.
- Ghosh, R.N., Gelman, D.L., Maxfield, F.R., 1994. Quantification of low-density lipoprotein and transferrin endocytotic sorting in hep2 cells using confocal microscopy. *J. Cell Sci.* 107, 2177–2189.
- Hao, M., Maxfield, F.R., 2000. Characterization of rapid membrane internalization and recycling. *J. Biol. Chem.* 275, 15279–15286.
- Heinrich, R., Rapoport, S.M., Rapoport, T.A., 1977. Metabolic regulation and mathematical models. *Prog. Biophys. Mol. Biol.* 32, 1–82.
- Helin, K., Beguinot, L., 1991. Internalization and down-regulation of the human epidermal growth factor receptor are regulated by the carboxyl-terminal tyrosines. *J. Biol. Chem.* 266, 8363–8368.
- Hill, T.A., 1942. The rate equations of consecutive reactions. *J. Am. Chem. Soc.* 64, 465–467.
- Lauffenburger, D.A., Linderman, J.J., 1993. *Receptors: Models for Binding, Trafficking and Signaling*. Oxford University Press, New York (Chapter 3).
- Levitzi, A., 1984. *Receptors, A Quantitative Approach*. Benjamin-Cummings, Menlo Park.
- Lin, C.C., Segel, L.A., 1988. *Mathematics Applied to Deterministic Problems in the Natural Sciences*. Society for Industrial and Applied Mathematics (SIAM), Philadelphia, pp. 303–320.
- Mukherjee, S., Ghosh, R.N., Maxfield, F.R., 1997. Endocytosis. *Physiol. Rev.* 77, 759–803.
- Mullick, A., Katzenellenbogen, B.S., 1986. Progesterone receptor synthesis and degradation in MCF-7 human breast cancer cells as studied by dense amino acid incorporation. Evidence for a non-hormone binding receptor precursor. *J. Biol. Chem.* 261, 13236–13246.
- Myers, A.C., Kovach, J.S., Vuk-Pavlovic, S., 1987. Binding, internalization, and intracellular processing of protein ligands. *J. Biol. Chem.* 262, 6494–6499.
- Opreško, L.K., Wiley, S.H., 1987. Receptor mediated endocytosis in *Xenopus* Oocytes. II. Evidence for two novel mechanisms of hormonal regulation. *J. Biol. Chem.* 262, 4116–4123.

- Ringerike, T., Stang, E., Johannessen, L.E., Sandnes, D., Levy, F.O., Madshus, I.H., 1998. High-affinity binding of epidermal growth factor (EGF) to EGF receptor is disrupted by overexpression of mutant dynamin (K44A). *J. Biol. Chem.* 273, 16639–16642.
- Roussel, M.R., Fraser, S.J., 1991. On the geometry of transient relaxation. *J. Chem. Phys.* 94, 7106–7113.
- Schauer, M., Heinrich, R., 1979. Analysis of the quasi-steady-state approximation for an enzymatic one-substrate reaction. *J. Theor. Biol.* 79, 425–442.
- Schnell, S., Maini, P.K., 2000. Enzyme kinetics at high enzyme concentration. *Bull. Math. Biol.* 62, 483–499.
- Schnell, S., Mendoza, C., 1997. A closed-form solution for time-dependent enzyme kinetic. *J. Theor. Biol.* 187, 207–212.
- Schnell, S., Mendoza, C., 2000a. Time-dependent closed form solution for fully competitive enzyme reactions. *Bull. Math. Biol.* 62, 321–336.
- Schnell, S., Mendoza, C., 2000b. Enzyme kinetics of multiple alternative substrates. *J. Math. Chem.* 27, 155–170.
- Schoeberl, B., Eichler-Jonsson, C., Gilles, E.D., Muller, G., 2002. Computational modeling of the dynamics of the MAP kinase cascade activated by surface and internalized EGF receptors. *Nature Biotech.* 20, 370–375.
- Shimizu, A., Kawashima, S., 1989. Kinetics of internalization and degradation of I-labeled follicle-stimulating hormone in mouse sertoli cells and its relevance to other systems. *J. Biol. Chem.* 264, 13632–13638.
- Sorkina, T., Huang, F., Beguinot, L., Sorkin, A., 2002. Effect of tyrosine kinase inhibitors on clathrin-coated pit recruitment and internalization of epidermal growth factor receptor. *J. Biol. Chem.* 277, 27433–27441.
- Starbuck, C., Lauffenburger, D.A., 1992. Mathematical model for the effects of epidermal growth factor receptor trafficking dynamics on fibroblast proliferation responses. *Biotechnol. Prog.* 8, 132–143.
- Swameye, I., Muller, T.G., Timmer, J., Sandra, O., Klingmuler, U., 2003. Identification of nucleocytoplasmic cycling as a remote sensor in cellular signaling by database modeling. *Proc. Natl Acad. Sci. USA* 100, 1028–1033.
- Tzafirri, A.R., 2003. Michaelis–menten enzyme kinetics at high enzyme concentrations. *Bull. Math. Biol.* 65, 1111–1129.
- Tzafirri, A.R., Edelman, E.R., 2004. The total quasi steady state approximation is valid for reversible enzyme kinetics. *J. Theor. Biol.* 226, 303–313.
- Tzafirri, A.R., Bercovier, M., Parnas, H., 2002. Reaction diffusion model of the enzymatic erosion of insoluble fibrillar matrices. *Biophys. J.* 83, 776–793.
- Wang, D., Lehman, R.E., Donner, D.B., Matli, M.R., Warren, R.S., Welton, M.L., 2002. Expression and endocytosis of VEGF and its receptors in human colonic vascular endothelial cells. *Am. J. Physiol. Gastrointest. Liver Physiol.* 282, G1088–G1096.
- Waters, C.M., Oberg, K.C., Carpenter, G., Overholser, K.A., 1990. Rate constants of binding, dissociation, and internalization of EGF: effect of receptor occupancy and ligand concentration. *Biochemistry* 29, 3563–3569.
- Wiley, S.H., Cunningham, D.D., 1981. A steady state model for analyzing the cellular binding, internalization and degradation of polypeptide ligands. *Cell.* 25, 433–440.
- Wiley, S.H., Cunningham, D.D., 1982. The endocytotic rate constant: a cellular parameter for quantifying receptor-mediated endocytosis. *J. Biol. Chem.* 257, 4222–4229.
- Wiley, S.H., Shvartsman, S.Y., Lauffenburger, D.A., 2003. Computational modeling of the EGF-receptor system: a paradigm for system biology. *Trends Cell Biol.* 13, 43–50.
- Zigmond, S., Sullivan, S.J., Lauffenburger, D.A., 1982. Kinetic analysis of chemotactic peptide receptor modulation. *J. Cell Biol.* 92, 34–43.